JOURNAL OF
THE INTERNATIONAL ASSOCIATION
FOR SHELL AND SPATIAL
STRUCTURES

Prof. D. h-C Eng. E. TORROJA, founder

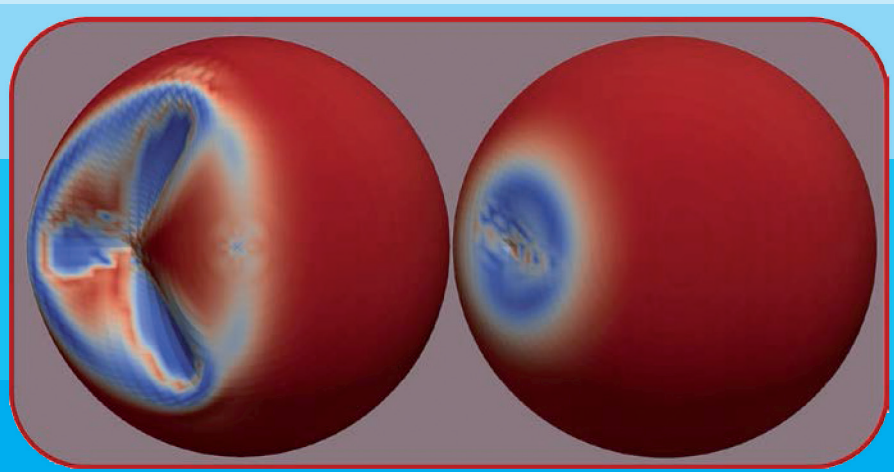

SPECIAL ISSUE
WG13 on:

COMPUTATIONAL METHODS FOR SHELL AND SPATIAL STRUCTURES

Guest Editors:
Makoto OHSAKI, Carlos LÁZARO and Kai-Uwe BLETZINGER

Vol. 62 (2021) No. 2
June n. 208
ISSN: 1028-365X

Journal

VOL. 62 (2021) No. 2
n. 208 June

contents

WG13 on "Computational Methods for Shell and Spatial Structures"

COVER: *Figure from paper by A. Niewiarowski, S. Adriaenssens and R. M. Pauletti*

IASS Secretariat: CEDEX-Laboratorio Central de Estructuras y Materiales
Alfonso XII, 3; 28014 Madrid, Spain
Tel: 34 91 3357491; Fax: 34 91 3357422; https://iass-structures.org
journal@iass-structures.org; iass@iass-structures.org
Printed by SODEGRAF ISSN:1028-365X Depósito legal: M. 1444-1960

Vol. 62 (2021) No. 2 June n. 208

SHAPE GENERATION OF BENDING-ACTIVE BRACED ARCHES BASED ON ELASTICA CURVES

JUAN BESSINI [1], SALVADOR MONLEÓN [2], JOSEP CASANOVA [3] and CARLOS LÁZARO [4]

[1]TYPSA Consulting Engineers & Architects, C/Botiguers, 5-5º, 46980 Paterna, Spain, jbessini@typsa.es
[2,3,4] Dep. Mecánica de Medios Continuos y T. E., Universitat Politècnica de València, Camino de Vera s/n, 46022 Valencia, Spain, smonleon@mes.upv.es, jcasano@mes.upv.es, carlafer@mes.upv.es (corresponding author)

Editor's Note: Manuscript submitted 26 January 2021; revision received 14 May 2021; accepted 26 May 2021. This paper is open for written discussion, which should be submitted to the IASS Secretariat no later than December 2021.

DOI: https://doi.org/10.20898/j.iass.2021.016

ABSTRACT

The active bending concept provides a new perspective for a well-established structural type which has been used at various scales: the beam-string, consisting of a beam with an attached lower tie in tension and bracing struts balancing the forces between them. The idea goes back to the gutter beams of the Crystal Palace and has been widely used to the present for large-scale structures. When a slender beam is used, the tension in the tie induces curvature in the beam and increases the structural depth of the system; this opens new formal possibilities and results in lightweight structures at the expense of increasing their overall flexibility. Systems of this kind fall within the realm of active bending. We name them bending-active braced arches. The target shape of the system follows the tensioning process and needs to be pre-determined by means of a specific analysis, typically involving dynamic relaxation or optimization-based methods. In this paper, we propose an analytical method to generate shapes for bending-active braced arches. It assumes that each segment of the activated rod between deviators behaves as a segment of elastica; this enables the use of closed-form expressions to evaluate the shape and induced stress level in the active member. Taking advantage of this idea, it is possible to devise a procedure to carry out the shaping process in a sequential way by adequately choosing the design parameters. When alternative choices for the parameters are selected, the problem becomes non-linear and can be solved using suitable techniques. Some examples with different design constraints have been reproduced to illustrate the possibilities of the method.

Keywords: *Bending-active structures, Beam-string system, Braced arch, Form finding, Euler's elastica*

1. INTRODUCTION

Curved shapes are often used to achieve better structural performance with less material consumption. Shells and arches are examples of this paradigm and have been successfully built with various materials throughout history. From the last quarter of the 20th century to our days a new way to erect curved structures has been introduced; it is based on using bending as the way to achieve curvature. Structures built by using this principle are called *bending-active structures*. In the core of the active bending concept, we recognize the advantageous idea of erecting a structure using the simplest possible building blocks: straight structural members pre-assembled on a flat surface; the assembly is pushed (or pulled) thereafter until the planned shape is achieved and the system is stabilized along the boundary and/or using additional structural members. There are excellent examples of domes built using this principle [1], [2], [3], [4]. Some of them are made of timber members; others use GFRP tubes, because of the high strength-to-rigidity ratio of these materials.

Looking back into the history of construction, we recognize a famous construction in which the bending-active principle was used, albeit in a less-spectacular way and for a very practical reason: we are referring to Paxton's Crystal Palace [5], built in 1851, and more specifically, to the gutter beams built therein (Paxton's gutters). They are U-shaped timber elements supported at both ends, with two cast-iron struts placed below and a lower tensioning wrought iron rod passing under them and attached to end shoes. The tension in the rod produced a pre-camber in the U-shaped timber element thanks to which water flowed to the drainage downpipes. The system

became a sort of inverted truss, much more rigid and strong than the original timber beam [6]. Large-scale and more complex versions of Paxton's gutter beam have been built all along the world, but without making use of active bending: we are referring to the so-called *beam-string* structural system, which has been successfully used for roofing structures and even bridges [7]. It consists of a beam with an attached lower tie in tension and bracing struts (deviators) balancing the forces between them.

If the beam of the beam-string system is very slender, the tension in the tie induces curvature in the beam, thereby changing the geometry of the system; this opens new formal possibilities and results in lightweight structures at the expense of an increased overall flexibility. Systems of this kind fall within the realm of active bending. We will refer to them as *bending-active braced (or tied) arches*: a simple planar structure composed of a continuous flexible member that is activated by the action of main cables pulling at both ends of the rod, and secondary struts (deviators) that deviate the main cable and act at certain cross-sections of the rod (Fig. 1). Secondary members will be referred to as deviators; they generally work in compression. The structure is activated by tensioning the cables and is stable under a certain state of self-stress. The geometry of the activated system cannot be fully prescribed in advance because it depends on the length and bending stiffness of the rod, as well as on the forces introduced by the deviators and the cable system.

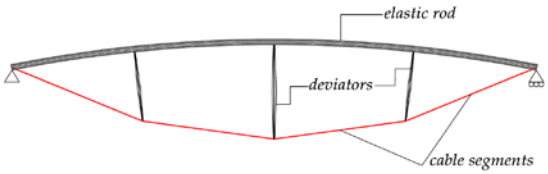

Figure 1: *Bending-active braced arch*

Configuration-finding constitutes a crucial part of the design process of bending-active structures and has been subject of intensive research in the last decades. Two main computational strategies have emerged: forward configuration search and inverse configuration search. The first one starts from stress-free flexible members which are pulled at certain locations by virtual cables or imposed movements to achieve a certain target shape by means of a non-linear FE simulation [8], [9]; the stress-free configuration must be defined in advance in a tentative process, often with the help of physical models. In the inverse configuration search strategy, a tentative deformed configuration, possibly (but not necessarily) close to the target, is first defined; then, it is relaxed to achieve equilibrium. This process is in many cases carried out with the Dynamic Relaxation strategy with a convenient underlying mechanical model, as in [10], [11], [12], [13], [14] to cite just some. In other cases, energy minimization [14], [15] or optimization techniques have been applied [14], [16].

This article deals with the configuration-finding of bending-active braced arches with an arbitrary number of deviators, including the shape and rigidity of the bent member, the geometry of deviators and the geometry and forces in the cables. Instead of using one of the general methods described in the previous paragraph, an analytical method oriented to this specific structural system has been developed. The flexible member is assumed to be made of a linear elastic material and to have segment-wise constant cross-section; axial and shear deformability are neglected. The self-weight of all structural elements is also neglected at this stage. With all these assumptions, equilibrium of structural members and nodes, and compatibility of rotations at nodes can be established in a straightforward way. The equilibrium configuration depends on the bending rigidity of the rod, but it is independent of the deformability of the cable and the deviators. The novelty resides in the fact that no limitation is posed to the magnitude of the deformation of the flexible member; therefore, instead of using the linear beam theory to model bending, the structural response of the flexible rod is modelled using Euler-Love's solution for the non-linear bending of a slender rod subject to end forces. The shape resulting from this theory is called *elastica* and has a closed but non-trivial mathematical expression. An alternative approach using the elastica theory was proposed by the authors in [17]. In addition, discrete approximations for the elastica were also used in [16] for shape finding of elastic gridshells.

Hence, our method starts from the fundamental assumption that each segment of the activated rod between deviators behaves as a segment of inflexional elastica. Consequently, to each elastica segment corresponds a cable segment, the axis of which joins the ideal inflexions of the corresponding elastica segment (Fig. 2). Of course, each segment of rod plus the corresponding cable segment "belong" to a different elastica, and the global shape follows from the compatibility of rotations at the nodes.

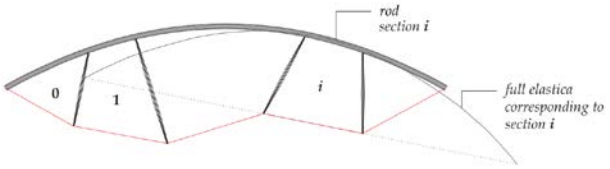

Figure 2: *Full (notional) elastica semi-wave corresponding to rod section i*

Taking advantage of this idea, it is possible to devise an analytical method to generate shapes for bending-active braced arches in a sequential way by adequately choosing the design parameters (initial data). Interestingly, in this case we can find solutions of the (non-linear) form-finding problem without solving any system of equations. However, in a general case, it may be convenient to choose a different set of initial parameters; then, the solution requires solving a system of non-linear equations.

The outline of the paper is as follows: in Section 2 we include a short review of Euler-Love's inflexional elastica and how elastica-shapes are scaled depending on the compressive force and the bending rigidity of the cross section. Section 3 starts with the definition of all design parameters, comprises the development of the equilibrium and compatibility equations and ends discussing the number of possible free initial parameters. Section 4 describes the direct method to generate equilibrium configurations in a sequential manner. Section 5 extends the method to consider form-finding problems with different constraints using an evolutionary solver. Both, Sections 4 and 5 include examples to demonstrate the application of the method. Finally, Section 6 concludes the article.

2. A BRIEF REVIEW OF THE INFLEXIONAL ELASTICA

The problem of planar bending of an initially straight rod subject to compressive forces at its ends, assuming non-extensibility and non-shear deformability, and neglecting self-weight is known as the elastica problem. It was first studied by Euler, based on Bernoulli's assumption of proportionality between flexural moments M and centerline curvatures κ at each cross-section. The full development of this theory can be found in the classical work by Love [18].

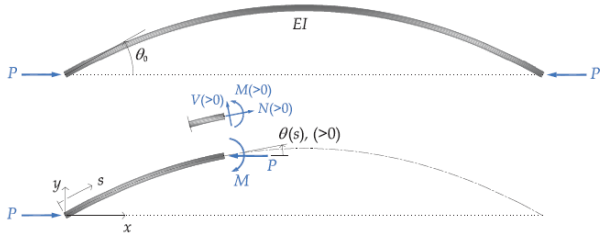

Figure 3: *Inflexional elastica. Defining variables*

The constitutive equation for the elastica is

$$M = EI\,\kappa \tag{1}$$

where the curvature is $\kappa = \mathrm{d}\theta/\mathrm{d}s$, s is an arc-length parameter, θ is the cross-section rotation and EI the flexural rigidity (Fig. 3). The analytical solution for the arc-length is:

$$s = \frac{1}{2}\sqrt{\frac{EI}{P}}\int_{-\theta_0}^{\theta}\frac{1}{\sqrt{\sin^2\frac{\theta_0}{2}-\sin^2\frac{\theta}{2}}}\,\mathrm{d}\theta \tag{2}$$

where P is the magnitude of the compressive force. The applicability of this expression is bounded into the interval $-\theta_0 \le \theta \le \theta_0$, where θ_0 is the cross-section rotation at the inflexion. To handle this issue, Love [18] introduced the variable ω, defined by:

$$\omega = \sin\frac{\theta}{2}\Big/\sin\frac{\theta_0}{2} \tag{3}$$

Substituting in (2), the expression for the arc-length reads as follows:

$$s = \sqrt{\frac{EI}{P}}\int_{-\pi/2}^{\omega}\frac{1}{\sqrt{1-k^2\sin^2\omega}}\,\mathrm{d}\omega \tag{4}$$

In this expression,

$$k = \sin\frac{\theta_0}{2} \tag{5}$$

is the reference parameter of the dimensionless solution of the elastica. The solution (4) can reproduce arbitrarily long elasticas because the new variable ω is not bounded. It can be expressed in terms of the *incomplete* and the *complete elliptic integrals of the first kind*:

$$\begin{aligned}\mathrm{F}(\omega,k) &= \int_0^{\omega}\frac{\mathrm{d}\omega}{\sqrt{1-k^2\sin^2\omega}}\\ \mathrm{K}(k) &= \int_{-\pi/2}^{0}\frac{\mathrm{d}\omega}{\sqrt{1-k^2\sin^2\omega}}\end{aligned} \tag{6}$$

as:

$$s(\omega,k)=\sqrt{\frac{EI}{P}}\left(\mathsf{F}(\omega,k)+\mathsf{K}(k)\right) \tag{7}$$

2.1. Geometry of the elastica

Using the *incomplete and complete elliptic integrals of the second kind*

$$\mathsf{E}(\omega,k)=\int_0^{\omega}\sqrt{1-k^2\sin^2\omega}\;\mathrm{d}\omega$$
$$\mathsf{E}(k)=\int_0^{\pi/2}\sqrt{1-k^2\sin^2\omega}\;\mathrm{d}\omega \tag{8}$$

the coordinates of the elastica are expressed as follows (note the difference in nomenclature between E and E):

$$x(\omega,k)=2\sqrt{\frac{EI}{P}}\left(\mathsf{E}(\omega,k)+\mathsf{E}(k)\right)-\mathrm{s}(\omega,k)$$
$$y(\omega,k)=2\sqrt{\frac{EI}{P}}\,k\cos\omega \tag{9}$$

2.2. Section forces

Normal forces and shear forces are obtained as projections of the compressive force, and bending moments as the product of the compressive force times the elastica ordinate:

$$N=-P\cos\theta$$
$$V=P\sin\theta \tag{10}$$
$$M=-Py$$

They can be expressed in terms of the elastica parameters as:

$$N(\omega,k)=-P(1-2k^2\sin^2\omega)$$
$$V(\omega,k)=-2Pk\sin\omega\sqrt{1-k^2\sin^2\omega} \tag{11}$$
$$M(\omega,k)=-2\sqrt{P}\sqrt{EI}\,k\cos\omega$$

2.3. Scalability of the solution

We introduce the parameter *critical length*:

$$l_c=\pi\sqrt{\frac{EI}{P}} \tag{12}$$

It is defined as the length of a rod with bending rigidity EI for which P is Euler's critical load —this definition was previously introduced by the authors in [17]. Using it, the arc-length and the coordinates of the elastica can be expressed as dimensionless quantities:

$$\zeta=s/l_c$$
$$\xi=x/l_c \tag{13}$$
$$\eta=y/l_c$$

Therefore, the non-dimensional arc-length parameter becomes:

$$\zeta(\omega,k)=\frac{1}{\pi}\left(\mathsf{F}(\omega,k)+\mathsf{K}(k)\right) \tag{14}$$

and the non-dimensional coordinates are:

$$\xi(\omega,k)=\frac{2}{\pi}\left(\mathsf{E}(\omega,k)+\mathsf{E}(k)\right)-\zeta(\omega,k)$$
$$\eta(\omega,k)=\frac{2}{\pi}k\cos\omega \tag{15}$$

These equations show that *the shape of an elastica is fully determined by the parameter* k (Eq. 5) —or in other words, by the angle at the inflexion (Fig. 4). On the other hand, *the size of the elastica is determined by the critical length* l_c, which acts as a scaling parameter.

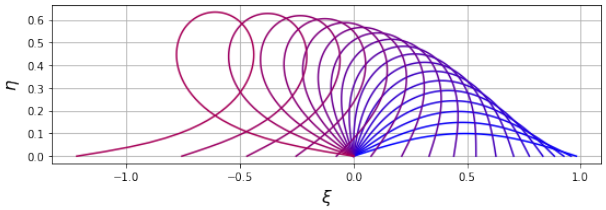

Figure 4: *Elasticas (in non-dimensional coordinates) for* $\theta_0=n\pi/20$ *and* $n\in\{2,3,\dots,17,18\}$

Finally, from equation (10) it can be noted that section forces N, V are directly scaled by the compressive force P, and bending moments M are scaled by the factor Pl_c/π.

To sum up, the *shape* of the elastica —defined by the parameter k— is fully determined by the angle at the inflexion θ_0 and is independent of the value of the compressive force P or the bending rigidity EI. Once the shape is obtained, the size of the elastica can be scaled by means of the critical length l_c (Eq. 12). It involves the relation between the bending rigidity EI and the compressive force P.

For example, once l_c has been fixed, the magnitude of the internal forces can be chosen by selecting P, and the bending rigidity EI should then be adjusted

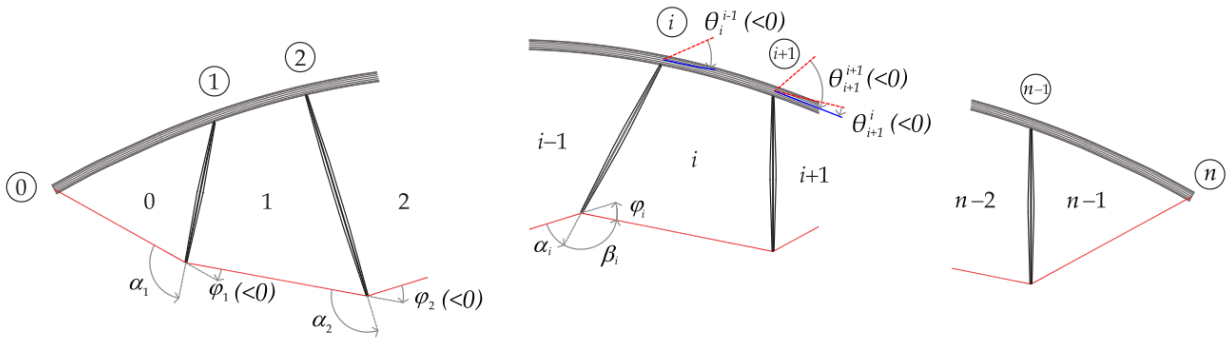

Figure 5: *Notation*

to be consistent with l_c:

$$EI = P\left(\frac{l_c}{\pi}\right)^2 \tag{16}$$

Alternatively, EI may be prescribed and the magnitude of the forces will be given by:

$$P = \pi^2 \frac{EI}{l_c^2} \tag{17}$$

3. SELF-STRESS STATES IN BENDING-ACTIVE TIED ARCHES

The simulation of the activation process of bending-active structures is of crucial importance for their design. Due to the non-linearity of the structural response, it is often not possible to predefine in advance the equilibrium configuration and computational form-finding methods are required for modelling the bending effect. However, in the case of bending-active tied arches, the fact that the rod segments between deviators behave as elastica segments enables the use of closed-form expressions to evaluate the stress level due to activation forces. The purpose of this section is to determine the sufficient and necessary conditions for obtaining the self-stress state of the arch using the equations of the exact solution of the elastica.

3.1. Notation

An intermediate node i on the rod separates two sections of the rod that are referred to as section $i-1$ and section i. Variables associated to the section i of the rod are denoted by the superscript i (Fig. 5).

Each section i of the rod is part of an elastica defined by the parameter k^i, the magnitude of the compressive force P^i and the flexural rigidity EI^i (see Fig. 2).

As each cable segment and the corresponding elastica section are in equilibrium, the compressive force acting on the elastica and the traction in the cable must have the same magnitude: $P^i = T^i$. Because of this, rod sections $i-1$ and i exert forces T^{i-1} and T^i (as well as moments M^{i-1} and M^i) on node i; these forces have the direction of the corresponding cable segments (see Fig. 6).

Angles between cable segments $i-1$, i and elastica tangents at each side of node i will be referred to as θ_i^{i-1} and θ_i^i. Therefore, a given elastica section i starts with an angle θ_i^i and ends with θ_{i+1}^i, both angles referred to the orientation of cable i. The ω variables (see Eq. (3)) corresponding to the elastica sections i and $i+1$ are ω_i^i and ω_{i+1}^i.

The angles formed by each cable segment $i-1$, i and the prolongation of the axis of the deviator are denoted α_i, β_i. The angular difference between cable segments is denoted as β_i. Then, the relation between angles at node i is:

$$\alpha_i + \beta_i + \varphi_i = \pi \tag{18}$$

3.2. Equilibrium and compatibility conditions at joints

Figure 6 shows the various equilibrium conditions at nodes. Equilibrium of moments at joints requires that $M_i^{i-1} = M_i^i$.

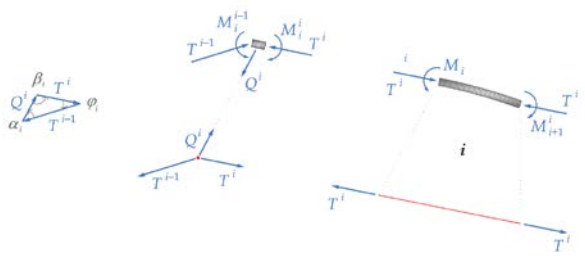

Figure 6: *Equilibrium of nodes and elastica sections (I)*

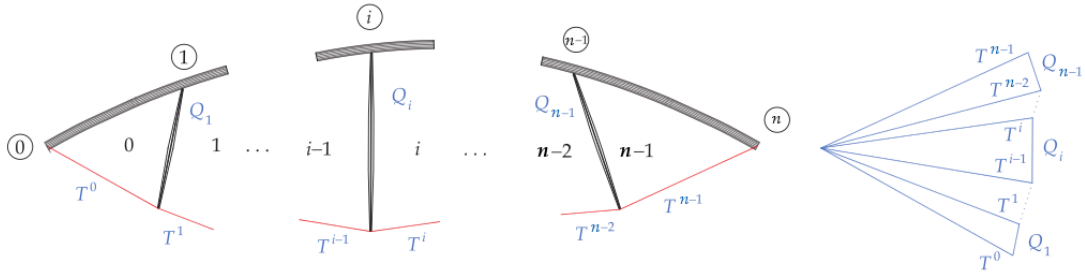

Figure 7: *Equilibrium of nodes and elastica sections (II)*

Substituting the expression for moments from Eq. (11):

$$\sqrt{T^{i-1}}\sqrt{EI^{i-1}}\,k^i\cos\omega_i^{i-1} = \sqrt{T^i}\sqrt{EI^i}\,k^i\cos\omega_i^i \tag{19}$$

equivalently:

$$T^{i-1}EI^{i-1}\left(k^{i-1}\right)^2\left(1-\sin^2\omega_i^{i-1}\right) = T^iEI^i\left(k^i\right)^2\left(1-\sin^2\omega_i^i\right) \tag{20}$$

Introducing the definition of ω and rearranging, the equilibrium condition can be expressed in terms of the rotations:

$$T^{i-1}EI^{i-1}\left(\left(k^{i-1}\right)^2-\sin^2\frac{\theta_i^{i-1}}{2}\right) = T^iEI^i\left(\left(k^i\right)^2-\sin^2\frac{\theta_i^i}{2}\right) \tag{21}$$

An alternative expression using critical lengths is:

$$\frac{1}{\pi^2}\left(T^{i-1}\right)^2\left(l_c^{i-1}\right)^2\left(\left(k^{i-1}\right)^2-\sin^2\frac{\theta_i^{i-1}}{2}\right) = \frac{1}{\pi^2}\left(T^i\right)^2\left(l_c^i\right)^2\left(\left(k^i\right)^2-\sin^2\frac{\theta_i^i}{2}\right) \tag{21}$$

The equilibrium of forces at each node on the elastica is defined by the compressive forces acting on each segment P^{i-1}, P^i and the force in the deviator Q_i. The triangle of forces at this node is the same as the triangle of forces at the corresponding node joining cable segments and deviator, acted by forces T^{i-1}, T^i, Q_i. The law of sines

$$\frac{T^{i-1}}{\sin\beta_i} = \frac{T^i}{\sin\alpha_i} = \frac{Q_i}{\sin\varphi_i} \tag{23}$$

leads to the following equilibrium equations:

$$T^{i-1}\sin\alpha_i = T^i\sin\beta_i$$
$$T^{i-1}\sin\varphi_i = Q_i\sin\beta_i \tag{24}$$

Compatibility of tangents to the elastica at both sides of a joint requires:

$$\theta_i^i = \theta_i^{i-1} + \varphi_i \tag{25}$$

A problem with n elastica sections, and therefore $n-1$ intermediate nodes in the rod, is considered. Following the previous discussion, the intervening variables are classified into three groups. The first group is reflected in Table 1 and gathers variables which are directly related to the self-stressing state: angles between cables and between deviators and cables, cable forces relative to the force in the first cable and deviator forces relative to the same magnitude. They can be visualized by means of a force polygon composed by cable forces and deviator forces (Fig. 7). Note that the choice of the magnitude of the force T^0 determines the scale of the force polygon.

Table 1: *Variables related to self-stressing forces*

Type	Notation		Number of variables
Angle	φ_i	$i \in \{1 \dots n-1\}$	$n-1$
Angle	α_i	$i \in \{1 \dots n-1\}$	$n-1$
Force	T^i/T^0	$i \in \{1 \dots n-1\}$	$n-1$
Force	Q^i/T^0	$i \in \{1 \dots n-1\}$	$n-1$
Total			$4(n-1)$

The second group (Table 2) comprises the variables that define the geometry (shape and relative size) of the sequence of elasticas: elastica parameters, critical lengths relative to the critical length of the first elastica section and angles at both sides of a node.

The third group (Table 3) is formed by the size and force scaling parameters: the critical length of the first elastica section and the force in the first cable.

Table 2: *Variables related to the form of the elastic rod*

Type	Notation		Number of variables
Angle	$\theta_i^{i-1}, \theta_i^i$	$i \in \{1 \dots n-1\}$	$2(n-1)$
Angle-related	k_i	$i \in \{0 \dots n-1\}$	n
Length	l_c^i / l_c^0	$i \in \{1 \dots n-1\}$	$n-1$
Total			$4(n-1)+1$

Table 3: *Size and force scaling variables*

Type	Notation	Number of variables
Length	l_c^0	1
Force	T^0	1
Total		2

Altogether, there are $8n-5$ variables defining the configuration: $4(n-1)$ self-stress related variables; $4(n-1)+1$ rod form related variables; one parameter l_c^0 to define the size of the structure, and one parameter T^0 to define the magnitude of internal forces and bending rigidity of the rod.

As for the equations, there are three equilibrium equations and one compatibility condition at each intermediate node of the rod (Table 4). This makes a total of $4(n-1)$ equations. Therefore, a given configuration is defined by choosing $4(n-1)+3$ parameters: $4(n-1)+1$ for determining the shape, one for setting the size and one for selecting the magnitude of forces and flexural rigidity of cross-sections.

Table 4: *Equilibrium and compatibility equations*

Type(*) / Eq. no.	Equation	Number of equations
E / (24)	$T^{i-1}\sin\alpha_i = T^i \sin\beta_i$	$n-1$
E / (24)	$T^{i-1}\sin\varphi_i = Q_i \sin\beta_i$	$n-1$
E / (21)	$(T^{i-1})^2 (l_c^{i-1})^2 \left((k^{i-1})^2 - \sin^2\frac{\theta_i^{i-1}}{2}\right) = (T^i)^2 (l_c^i)^2 \left((k^i)^2 - \sin^2\frac{\theta_i^i}{2}\right)$	$n-1$
C / (25)	$\theta_i^i = \theta_i^{i-1} + \varphi_i$	$n-1$
Total		$4(n-1)$

(*) E means equilibrium; C means compatibility.

4. DIRECT DETERMINATION OF SELF-STRESS CONFIGURATIONS

In this section a direct method to obtain self-stress configurations of bending-active tied arches is presented. This method is direct in the sense that a solution for the $4(n-1)$ unknowns is obtained in a sequential manner, after selecting $4(n-1)+3 = 4n-1$ parameters and does not require to solve any system of equations.

Observing that the $2(n-1)$ force equilibrium equations (24) at intermediate nodes only involve the $4(\mathrm{n}-1)$ self-stress related variables of Table 1, the following procedure solves the problem:

1. Define a value for T^0.
2. Define values for α_i, φ_i, $i \in \{1 \dots n-1\}$. In this step, $2(n-1)$ parameters are set.
3. Compute T^i and Q_i for, $i \in \{1 \dots n-1\}$ using force equilibrium equations (24). This is a direct computation considering that $\beta_i = \pi - \alpha_i - \phi_i$.
4. Define values for θ_i^{i-1}, $i \in \{1 \dots n-1\}$. With this step $n-1$ parameters are additionally set.
5. Compute θ_i^i using compatibility equations (25).
6. Define values for k_0 and EI^i for $i \in \{0 \dots n-1\}$. This step sets $n+1$ additional parameters.
7. Compute k_i for $i \in \{1 \dots n-1\}$ using moment equilibrium equations (21).
8. Compute local coordinates of elastica i using equations (9).
9. Place each elastica segment by translating it to the end of the previous one and rotating it to preserve tangents at intermediate nodes.

It is worth noting that steps 1 to 3 are equivalent to the definition of the force polygon that corresponds to the system of cables and deviators. This graphical approach has been already used by Boulic *et al.* [19], who proposed a graphical method for the design of hybrid bending-active structures composed of active elements with non-constant stiffness and tensile cable nets. Particularly, their method makes use of a force diagram to obtain the non-constant distribution of bending rigidity along the active members for a certain target bent geometry under given loads.

Step 5 requires checking that angle θ_i^i is smaller than θ_{i-1}^i. If this condition is not met, the elastica i will be wrongly computed with a reversed orientation; to

avoid this, 2π should be added to θ_i^i. In step 6, k_0 is related to the angle between cable and elastica tangent at the start of the structure. In addition, setting the n values of flexural rigidity EI^i is equivalent to setting the n values of critical length l_c^i because forces T^i are already known.

Once a configuration is found, its size and the magnitude of the forces can be adjusted to the desired values by changing EI^0 and T^0.

A convenient procedure is to initially set $T^0 = 1$ and $EI^0 = 1/\pi^2$, so that $l_c^0 = 1$. After computing the solution and the coordinates of the structure, the size of the structure can be scaled to the desired value. If the scale factor is assumed as l; then the first critical length shall be $l_c^0 = l$. If $EI^0 = EI$ is chosen as a desired value, then all forces shall be scaled by $T^0 = \pi^2 EI/l^2$. Another possibility is to choose the magnitude of forces by setting $T^0 = T$ and then obtain the required flexural rigidity scale factor as $EI^0 = Tl^2/\pi^2$. Table 5 summarizes the prescribed variables and the computed variables for this direct method.

Table 5: *Prescribed and computed variables in the direct method*

Prescribed		Computed	
Variable	Number	Variable	Number
T^0	1	T^i	$n-1$
φ_i	$n-1$	Q_i	$n-1$
α_i	$n-1$		
θ_i^{i-1}	$n-1$	θ_i^i	$n-1$
k^0	1		
EI^i	n	k^i	$n-1$
Total	$4n-1$	Total	$4n-4$

4.1. Examples

Generic case. A generic case with $n = 5$ elastica sections generated with the sequential procedure is shown in Fig. 8.

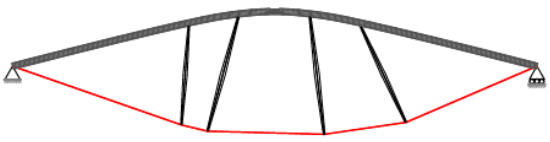

Figure 8: *Example of a generic structure with $n = 5$ elastica sections shaped with the sequential method*

Initial prescribed parameters are $T^0 = 1$ and $EI^i = 1/\pi^2$ for all i. Then, a set of angles α_i and φ_i, together with k^0 have been chosen (The value of k^0 corresponds to an initial angle $\theta_0 = 40$ deg.) Their values and the remaining parameters, calculated with the sequential procedure, are included in Table 6.

Perpendicular deviators. Perpendicularity between deviators and rod can be prescribed adding the following condition:

$$\theta_i^{i-1} = \pi/2 + \alpha_i \tag{26}$$

The result is represented in Fig. 9.

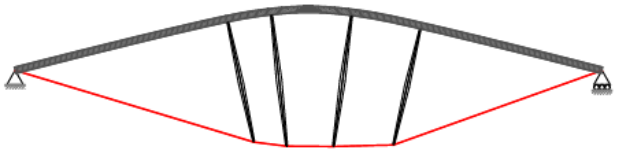

Figure 9: *Generic bending-active tied arch with $n = 5$ elastica sections and perpendicular deviators*

Symmetric structure with even number of rod sections. The following additional conditions lead to a symmetric solution for an even number n of elastica sections:

- Conditions on the polygon of forces:

$$\begin{aligned} &\varphi_{n-i} = \varphi_i && i \in \{1 \dots n/2-1\} \\ &\alpha_{n/2} = (\pi - \varphi_{n/2})/2 && \\ &\alpha_{n-i} = \pi - \varphi_i - \alpha_i && i \in \{1 \dots n/2-1\} \end{aligned} \tag{27}$$

- Conditions on the geometry of the rod:

$$\begin{aligned} &\theta_{n-i}^{n-i-1} = -\theta_i^i && i \in \{1 \dots n/2-1\} \\ &\theta_{n/2}^{n/2-1} = -\varphi_{n/2}/2 && \\ &EI^{n-i-1} = EI^i && i \in \{1 \dots n/2-1\} \end{aligned} \tag{28}$$

Therefore, symmetry adds $n-1$ conditions to the force polygon and n conditions to the form of the rod. This leaves $(4n-1)-(2n-1) = 2n$ free variables to determine a configuration. (A different approach to symmetry would be to reduce the number of unknowns and equations from scratch.) In the symmetric case with even number of elastica sections there are $4n-2$ variables.

Table 6: *Prescribed variables and computed unknowns for the generic case*

Variable	Prescribed	Computed	Variable	Prescribed	Computed
T^0	1		θ_1^0	$30\pi/180$	
T^1		0.9430	θ_2^1	$10\pi/180$	
T^2		0.9623	θ_3^2	$-5\pi/180$	
T^3		0.9595	θ_4^3	$-15\pi/180$	
T^4		0.8601	θ_1^1		0.2616
Q_1		0.2600	θ_2^2		0.0435
Q_2		0.1261	θ_3^3		-0.1742
Q_3		0.1258	θ_4^4		-0.5229
Q_4		0.2572	k^0	$\sin\left(\frac{1}{2}\cdot\frac{40\pi}{180}\right)$	
φ_1	$-15\pi/180$		k^1		0.2645
φ_2	$-7.5\pi/180$		k^2		0.2482
φ_3	$-7.5\pi/180$		k^3		0.2625
φ_4	$-15\pi/180$		k^4		0.3532
α_1	$-70\pi/180$		EI^0	$1/\pi^2$	
α_2	$-95\pi/180$		EI^1	$1/\pi^2$	
α_3	$-275\pi/180$		EI^2	$1/\pi^2$	
α_4	$-60\pi/180$		EI^3	$1/\pi^2$	
			EI^4	$1/\pi^2$	

Table 7: *Prescribed variables and computed unknowns corresponding to the generic case with perpendicular deviators*

Variable	Prescribed	Computed	Variable	Prescribed	Computed
T^0	1		θ_1^0	$30\pi/180$	
T^1		0.8964	θ_2^1	$10\pi/180$	
T^2		0.8836	θ_3^2	$-5\pi/180$	
T^3		0.9016	θ_4^3	$-15\pi/180$	
T^4		1.0056	θ_1^1		0.2616
Q_1		0.2681	θ_2^2		0.0435
Q_2		0.1172	θ_3^3		-0.2182
Q_3		0.1182	θ_4^4		-0.5229
Q_4		0.2696	k^0	$\sin\left(\frac{1}{2}\cdot\frac{40\pi}{180}\right)$	
φ_1	$-15\pi/180$		k^1		0.2697
φ_2	$-7.5\pi/180$		k^2		0.2580
φ_3	$-7.5\pi/180$		k^3		0.2743
φ_4	$-15\pi/180$		k^4		0.3451
α_1		-1.0471	EI^0	$1/\pi^2$	
α_2		-1.3962	EI^1	$1/\pi^2$	
α_3		-1.6579	EI^2	$1/\pi^2$	
α_4		-1.8316	EI^3	$1/\pi^2$	
			EI^4	$1/\pi^2$	

Table 8 shows the splitting between prescribed and computed variables with the direct method. The equations and their number are shown in Table 9.

Table 8: *Prescribed and computed variables in a symmetric structure with even number of elastica sections (direct method)*

Prescribed		Computed	
Variable	Number	Variable	Number
T^0	1	T^i	$n/2-1$
φ_i	$n/2$	Q_i	$n/2$
α_i	$n/2-1$	$\alpha_{n/2}$	1
θ_i^{i-1}	$n/2-1$	$\theta_{n/2}^{n/2-1}$	1
k^0	1	θ_i^i	$n/2-1$
EI^i	$n/2$	k^i	$n/2-1$
Total	$2n$	Total	$2n-4$

Let's consider a structure with $n=4$ rod sections. Table 10 includes the $2n=8$ prescribed parameters and the $2n-1=7$ computed unknowns following the procedure described in the preceding section. The resulting geometry is represented in Figure 10.

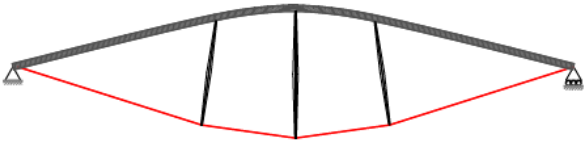

Figure 10: *Symmetric bending-active tied arch with $n=4$ elastica sections*

Table 9: *Equations in a symmetric structure with even number of rod sections*

Type(*) / Eq. no.	Equation	Number of equations
E / (24)	$T^{i-1}\sin\alpha_i = T^i \sin\beta_i$	$n/2-1$
E / (24)	$T^{i-1}\sin\varphi_i = Q_i \sin\beta_i$	$n/2-1$
S / (27)	$\alpha_{n/2} = (\pi - \varphi_{n/2})/2$	1
E / (24)	$T^{n/2-1}\sin\varphi_{n/2} = Q_{n/2}\sin\beta_{n/2}$	1
E / (21)	$(T^{i-1})^2(l_c^{i-1})^2\left((k^{i-1})^2 - \sin^2\frac{\theta_i^{i-1}}{2}\right) = (T^i)^2(l_c^i)^2\left((k^i)^2 - \sin^2\frac{\theta_i^i}{2}\right)$	$n/2-1$
C / (25)	$\theta_i^i = \theta_i^{i-1} + \varphi_i$	$n/2-1$
S / (28)	$\theta_{n/2}^{n/2-1} = -\varphi_{n/2}/2$	1
Total		$2n-1$

(*) E means equilibrium; C means compatibility; S means symmetry.

Table 10: *Prescribed variables and computed unknowns in the symmetric example*

Variable	Prescribed	Computed	Variable	Prescribed	Computed
T^0	1		θ_1^0	$30\pi/180$	
T^1		0.9659	θ_1^1		0.2617
Q_1		-0.2588	θ_2^1		0.0654
Q_2		-0.1263	k^0	$\sin\left(\frac{1}{2}\cdot\frac{40\pi}{180}\right)$	
φ_1	$-15\pi/180$		k^1		0.2622
φ_2	$-7.5\pi/180$		EI^1	$1/\pi^2$	
α_1	$105\pi/180$		EI^0	$1/\pi^2$	
α_2		1.6362			

Symmetric structure with odd number of rod sections. This case can be solved using the following additional constraints:

$$\begin{aligned} &\varphi_{n-i} = \varphi_i && i \in \{1 \dots (n-1)/2\} \\ &\alpha_{n-i} = \pi - \varphi_i - \alpha_i && i \in \{1 \dots (n-1)/2\} \\ &\theta_{n-i}^{n-i-1} = -\theta_i^i && i \in \{1 \dots (n-1)/2\} \\ &EI^{n-i-1} = EI^i && i \in \{1 \dots (n-1)/2\} \end{aligned} \quad (29)$$

Alternatively, a reduced number of variables and equations can be used. Variables and equations can be found in Tables 11 and 12.

Table 11: *Prescribed and computed variables in a symmetric structure with odd number of elastica sections (direct method)*

Prescribed		Computed	
Variable	Number	Variable	Number
T^0	1	T^i	$(n-1)/2$
φ_i	$(n-1)/2$	Q_i	$(n-1)/2$
α_i	$(n-1)/2$		
θ_i^{i-1}	$(n-1)/2$		
k^0	1	θ_i^i	$(n-1)/2$
EI^i	$(n+1)/2$	k^i	$(n-1)/2$
Total	$2n+1$	Total	$2n-2$

Table 12: *Equations in a symmetric structure with odd number of rod sections*

Type(*) / Eq. no.	Equation	Number of equations
E / (24)	$T^{i-1} \sin\alpha_i = T^i \sin\beta_i$	$(n-1)/2$
E / (24)	$T^{i-1} \sin\varphi_i = Q_i \sin\beta_i$	$(n-1)/2$
E / (21)	$(T^{i-1})^2 (l_c^{i-1})^2 \left((k^{i-1})^2 - \sin^2\frac{\theta_i^{i-1}}{2}\right) = (T^i)^2 (l_c^i)^2 \left((k^i)^2 - \sin^2\frac{\theta_i^i}{2}\right)$	$(n-1)/2$
C / (25)	$\theta_i^i = \theta_i^{i-1} + \varphi_i$	$(n-1)/2$
Total		$2n-2$

(*) E means equilibrium; C means compatibility.

5. COMPUTATION OF SELF-STRESS CONFIGURATIONS UNDER ADDITIONAL CONSTRAINTS

In Section 4 it was shown that $4(n-1)+3 = 4n-1$ variables can be independently selected in a general case.

The remaining $4(n-1) = 4n-4$ unknown variables that define a configuration can be calculated using the same number of equations: $3(n-1)$ equilibrium and $n-1$ compatibility equations.

If additional constraints are imposed, the number of independent parameters decreases. For instance, when searching symmetric configurations or solutions with perpendicularity between rod and deviators (see previous section). Moreover, when the choice of parameters is different from the one explained in Section 4, the problem non-linearity requires suitable solution techniques.

Among the set of search strategies, heuristic algorithms are well known for providing good approximate solutions to problems that cannot be solved easily using other techniques. Within heuristics, evolutionary algorithms have been deeply developed in the last decade. They mimic the theory of evolution using the same trial-and-error procedures that nature uses to arrive at an optimized outcome. Using this idea, Rutten [20] created a tool called Galapagos, which facilitates this process within *Grasshopper* (a graphical algorithm editor). Starting from the definition of the form-finding variables and constraints, this evolutionary solver finds the solution of the problem (or at least, a near-optimal solution) in an iterative manner. In the following, we present three examples to illustrate the method.

Example 1. In this first example, the target is to find the shape of a symmetric bending active arch with four rod sections n = 4 of equal flexural rigidity and length. Cable forces are prescribed, as well as the angle between first cable and first tangent to the rod.

Firstly, it will be checked that the number of prescribed variables and conditions allows to find a solution. As shown in the previous section, a symmetric bending active arch with even number of rod sections leaves $2n = 8$ parameters to be chosen. $T^0 = 1$ and $EI^0 = 1/\pi^2$ are chosen as starting values; they will be adjusted at the end of the process to achieve the desired size of the structure. This leaves freedom to define six additional

parameters and/or conditions. Once T^0 has been chosen, the other forces T^1, Q_0 and Q_1 and the angle α_2 are determined if the angles φ_1, φ_2 and α_1 are selected, as shown in the example of the previous section. Table 13 shows the values of angles and forces.

Three conditions remain to be set to find the solution:

- The angle between the first cable and the first tangent:

$$\theta_0^0 = -40\pi/180 \tag{30}$$

Therefore:

$$k^0 = \sin\left(\frac{1}{2}\frac{40\pi}{180}\right) \tag{31}$$

- Equal flexural rigidity in all rod sections: $n/2 - 1 = 1$ condition.

$$EI^1 = EI^0 (= 1) \tag{32}$$

- Equal length in all rod sections: $n/2 - 1 = 1$ condition.

$$l^1 = l^0 \tag{33}$$

From Eq. (7), the lengths of each elastica segment can be expressed as follows:

$$\begin{aligned} l^0 &= \sqrt{\frac{EI^0}{T^0}}\left(\mathrm{F}(\omega_1^0, k^0) + \mathrm{K}(k^0)\right) \\ l^1 &= \sqrt{\frac{EI^1}{T^1}}\left(\mathrm{F}(\omega_2^1, k^1) - \mathrm{F}(\omega_1^1, k^1)\right) \end{aligned} \tag{34}$$

Therefore, from Eqs. (33) and (34):

$$\begin{aligned} T^1\left(\mathrm{F}(\omega_1^0, k^0) + \mathrm{K}(k^0)\right) \\ - T^0\left(\mathrm{F}(\omega_2^1, k^1)\right. \\ \left. - \mathrm{F}(\omega_1^1, k^1)\right) = 0 \end{aligned} \tag{35}$$

with:

$$\begin{aligned} \sin\omega_1^0 &= \frac{1}{k^0}\sin\frac{\theta_1^0}{2} \\ \sin\omega_1^1 &= \frac{1}{k^1}\sin\frac{\theta_1^1}{2} \\ \sin\omega_2^1 &= \frac{1}{k^1}\sin\frac{\theta_2^1}{2} \end{aligned} \tag{36}$$

The previous equations together with: (a) the moment equilibrium equation; (b) the compatibility condition in node 1 and (c) the symmetry condition in node 2,

$$\begin{aligned} T^0(k^0)^2(1 - \sin^2\omega_1^0) \\ - T^1(k^1)^2(1 - \sin^2\omega_1^1) \\ = 0 \end{aligned}$$

$$\theta_1^1 = \theta_1^0 - \varphi_1 \tag{37}$$

$$\theta_2^1 = \varphi_2/2$$

allow to calculate the four unknowns θ_1^0, θ_1^1, θ_2^1 and k^1. In this case, the solution has been found iterating over θ_1^0 using the plug-in *Galapagos* until:

$$l^1 - l^0 = 0 \tag{38}$$

The result is shown in Fig. 11 and Table 13.

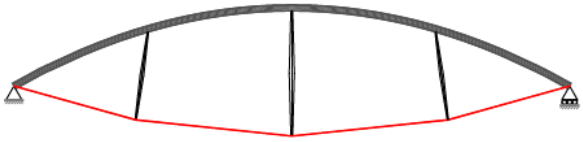

Figure 11: *Symmetric bending-active tied arch with $n = 4$ elastica sections of equal length (Example 1)*

Example 2. Here, the objective is to reproduce the first example adding the condition of perpendicularity between deviators and rod. Due to this condition, the solution can be found iterating over α_1 instead of θ_1^0. The solution is shown in Fig. 12 and Table 14.

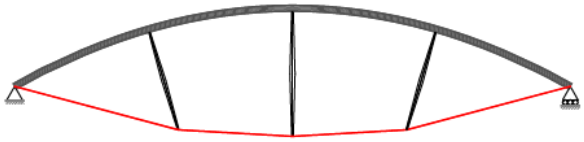

Figure 12: *Symmetric bending-active tied arch with $n = 4$ elastica sections corresponding to Example 2*

Example 3. In the last example, the purpose is to form-find the shape of a symmetric bending active arch with $n = 5$ rod sections, with perpendicular deviators and same distance between deviator-rod joints projected over the x-axis. The cable and rod forces as well as the angle between first cable and first tangent to the rod are prescribed. Relations EI^0/EI^1 and EI^0/EI^2 are iteratively searched in two steps using Galapagos until the following conditions are met:

$$\frac{d_x^1}{d_x^0} = \frac{x^2 - x^1}{x^1 - x^0} = 1$$
$$d_x^2 = d_x^0/2 \qquad (38)$$

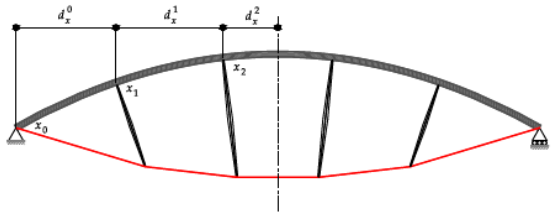

Figure 13: *Symmetric bending-active tied arch with $n = 5$ elastica sections corresponding to Example 3*

6. CONCLUSION

We have developed an analytical method to find the configuration of bending-active braced arches. They are a hybrid between a tied arch and a cable-strut beam: a planar structure composed of a continuous flexible rod that is activated by the action of lower ties (cables) and secondary struts that deviate the tie sections and provide balance between rod and ties. The target shape of the system is achieved as a result of the tensioning process. As the problem is non-linear, it cannot be specified *a priori*.

Neglecting self-weight of the structure, right after the activation, each section of the flexible rod in the braced arch is acted by a constant compressive force; this force has the same direction as the corresponding section of cable. Consequently, we may assume that each rod section behaves as part of an inflexional *elastica* if shear and axial deformation are neglected.

Using Love's closed-form solution of Euler's *elastica* theory, it is possible to systematically formulate the equilibrium and compatibility equations of the system to determine the shape and induced internal forces in the rod, struts and cables after the activation.

A sequential calculation process based on the scalability of solutions and on a suitable choice of free design parameters allows to determine all design variables without solving non-linear equations. Several examples have been included to illustrate the sequential process. When other sets of design parameters are selected, the problem requires the solution of a non-linear system of equations. We have used a heuristic algorithm to solve the resulting system, and some examples with different design constraints have been included to show the possibilities of the method to define self-stressed configurations.

The proposed method has been specifically designed for a particular structural type. The lack of generality is compensated by its efficiency: the fact that closed solutions of the non-linear form finding problem can be directly obtained by means of a sequential process allows a fast and accurate generation of self-stressed shapes. This makes it especially suitable for applying heuristic tools to direct the search of optimal configurations for this lightweight structural system. Finally, although the direct extension of this method for general 3D configurations is not possible (as there are no general closed-form expressions for the 3D elastica curve), it could be applicable for approximating spatial configurations where the out-of-plane deformation is small.

Table 13: *Prescribed variables and computed unknowns in Example 1 (Section 5)*

Variable	Prescribed	Computed	Variable	Prescribed	Computed
T^0	1		θ_1^1		0.3202
T^1		0.9659	θ_2^1		0.0654
Q_1		-0.2645	θ_1^0		0.5880
Q_2		-0.1262	k^0	$\sin\left(\frac{1}{2}\cdot\frac{40\pi}{180}\right)$	
φ_1	$-15\pi/180$		k^1		0.2440
φ_2	$-7.5\pi/180$		EI^1	$1/\pi^2$	
α_1	$105\pi/180$		EI^0	$1/\pi^2$	
α_2		1.6361			

Table 14: *Prescribed variables and computed unknowns in Example 2 (Section 5)*

Variable	Prescribed	Computed	Variable	Prescribed	Computed
T^0	1		θ_1^0		0.5868
T^1		0.8769	θ_1^1		0.3191
Q_1		0.2785	θ_2^1		0.0654
Q_2		-0.1460	k^0	$\sin\left(\frac{1}{2}\cdot\frac{40\pi}{180}\right)$	
φ_1	$-15\pi/180$		k^1		0.2513
φ_2	$-7.5\pi/180$		EI^1	$1/\pi^2$	
α_1		-0.9839	EI^0	$1/\pi^2$	
α_2		1.6361			

Table 15: *Prescribed variables and computed unknowns in Example 3 (Section 5)*

Variable	Prescribed	Computed	Variable	Prescribed	Computed
T^0	1		θ_1^0		0.5236
T^1		0.8963	θ_1^1		0.2609
T^2		0.8835	θ_2^1		0.1745
Q_1		0.2688	θ_2^2		0.0432
Q_2		0.1174	k^0	$\sin\left(\frac{1}{2}\cdot\frac{40\pi}{180}\right)$	
φ_1	$-15\pi/180$		k^1		0.1719
φ_2	$-7.5\pi/180$		k^2		0.1423
α_1	$-60\pi/180$		EI^0	$1/\pi^2$	
α_2	$-80\pi/180$		EI^1		0.4466
			EI^2		0.5029

ACKNOWLEDGMENTS

This work has been partially supported by the Spanish Ministry of Economy and Competitiveness through grant BIA2015-69330-P (MINECO).

REFERENCES

[1] E. Happold and W. Liddell, "Timber lattice roof for the Mannheim Bundesgartenschau," *The Structural Engineer*, vol. 53-3, pp. 99-135, 1975.

[2] M. McQuaid, F. Otto and S. Ban, "Building the Japan pavilion," in *Shigeru Ban*, Phaidon Press, 2006, pp. 8-11.

[3] R. Harris and O. Kelly, "The structural engineering of the Downland gridshell," in *Space Structures 5*, G. A. R. Parke and P. Disney, Eds., Thomas Telford, 2002, pp. 161-172. (DOI: 10.1680/ss5v1.31739.0018)

[4] L. du Peloux, J-F. Caron, F. Tayeb, O. Baverel, "The ephemeral cathedral of Créteil: a 350m2 lightweight structure made of a GFRP composite gridshell," in *CIGOS 2015: Innovations in Construction*, CIGOS, Cachan, France, May 11th-12th, 2015

[5] B. Addis, "The Crystal Palace and its Place in Structural History," *International Journal of Space Structures*, vol. 21-1, pp. 3-19, 2006. (DOI:10.1260/026635106777641199)

[6] P. Berlyn and C. Fowler, *The Crystal Palace: Its Architectural History and Constructing Marvels*, London: James Gilbert (Publisher), 1851.

[7] M. Saitoh, "40 years after-development and possibility of beam string structures," in *Form and Force: Proceedings of the IASS Annual Symposium – Structural Membranes 2019*, Barcelona, Spain, October 7th-10th, 2019.

[8] J. Lienhard, R. La Magna and J. Knippers, "Form-finding bending-active structures with temporary ultra-elastic contraction elements," *WIT Transactions on the Built Environment*, vol. 136, pp. 107-116, 2014. (DOI: 10.2495/MAR140091)

[9] J. Rombouts, G. Lombaert, L. De Laet, M. Schevenels, "A novel shape optimization approach for strained gridshells: Design and construction of a simply supported gridshell," *Engineering Structures*, vol. 192, pp. 166-180, 2019. (DOI: 10.1016/j.engstruct.2019.04.101)

[10] S. Adriaenssens and M. R. Barnes, "Tensegrity spline beam and grid shell structures," *Engineering Structures*, vol. 23, no. 1, pp. 29-36, 2001. (DOI: 10.1016/S0141-0296(00)00019-5)

[11] M. R. Barnes, S. Adriaenssens, M. Krupka, "A novel torsion/bending element for dynamic relaxation modelling," *Computers and Structures*, vol. 119, pp. 60-67, 2013. (DOI: 10.1016/j.compstruc.2012.12.027)

[12] B. D'Amico, A. Kermani, H. Zhang, "Form finding and structural analysis of actively bent timber grid shells," *Engineering Structures*, vol. 81, pp. 195-207, 2014. (DOI: 10.1016/j.engstruct.2014.09.043)

[13] J. Bessini, C. Lázaro, S. Monleón, "A form-finding method based on the geometrically exact rod model for bending-active structures," *Engineering Structures*, vol. 152, pp. 549-558, 2017. (DOI: 10.1016/j.engstruct.2017.09.045)

[14] Y. Sakai, M. Ohsaki, S. Adriaenssens, "A 3-dimensional elastic beam model for form-finding of bending-active gridhsells," *International Journal of Solids and Structures*, vol. 193-194, pp. 328-337, 2020. (DOI: 10.1016/j.ijsolstr.2020.02.034)

[15] A. M. Bauer, R. Wüchner and K.-U. Bletzinger, "Isogeometric analysis in the design process of lightweight structures," in *Form and Force: Proceedings of the IASS Annual Symposium – Structural Membranes 2019*, Barcelona, Spain, October 7th-10th, 2019.

[16] Y. Sakai and M. Ohsaki, "Discrete elastica for shape design of gridshells," *Engineering Structures*, vol.169, pp. 55-67, 2018. (DOI: 10.1016/j.engstruct.2018.05.002)

[17] C. Lázaro, S. Monleón and J. Casanova, "Can the force density method be extended for active bending structures?" in *Future Visions: Proceedings of the IASS Annual Symposium 2015*, Amsterdam, The Netherlands, 2015.

[18] AEH. Love, *A Treatise on the Mathematical Theory of Elasticity*. New York: Dover, 1944.

[19] L. Boulic and J. Schwartz, "Design Strategies of Hybrid Bending-Active Systems Based on Graphic Statics and a Constrained Force Density Method," *Journal of the International Association for Shell and Spatial Structures*, vol. 59-4, pp. 267-275, 2018. (DOI: 10.20898/j.iass.2018.198.038)

[20] D. Rutten, "Galapagos: On the Logic and Limitations of Generic Solvers", *Architectural Design*, vol. 83, pp. 132-135, 2013. (DOI: 10.1002/ad.1568)